Int. J. Therm. Sci. (2000) 39, 1004–1014

S1290-0729(00)01172-8/FLA

The formation and behavior of fog in a tube bundle condenser

Arne Manthey, Karlheinz Schaber *

Institut für Technische Thermodynamik und Kältetechnik, Universität Karlsruhe, D-76128 Karlsruhe, Germany

(Received 12 May 2000, accepted 13 July 2000)

Dedicated to Prof. Dr.-Ing. Dr. h.c. mult. Karl Stephan on the occasion of his 70th birthday

Abstract — The formation and behavior of fog during partial condensation of humid air in a vertical tube bundle condenser has been investigated. For this purpose a special glass condenser has been constructed which allows to measure the aerosol parameters everywhere along the cooling tubes using an optical aerosol measurement system. At the operation conditions adjusted in the present work fog occurs only in the presence of foreign nuclei by heterogeneous nucleation. It is shown, that the total mass of fog being formed was not influenced by the number concentration of foreign nuclei. The formation of fog occurs immediately after the first contact of the humid air with the cooling wall due to local supersaturation. After the fog has been formed in the entry of the condenser, a strong decrease of fog particles has been observed further down with the total amount of fog being constant. The effect of various process settings on the resulting aerosol parameters has been investigated. Both simple and rigorous one-dimensional calculations and complex multi-dimensional simulations using CFD were carried out for the interpretation of experimental data. Although the multi-dimensional simulations showed strong local effects the one-dimensional models were suitable to predict the conditions for fog formation. © 2000 Éditions scientifiques et médicales Elsevier SAS

aerosol / fog / partial condensation / heterogeneous nucleation

Nomenclature

c_p	heat capacity	$J \cdot kg^{-1} \cdot K^{-1}$
d_{NV}	number volume averaged diameter	μm
D	binary diffusion coefficient of vapor molecules in the inert gas	$m^2 \cdot s^{-1}$
J	nucleation rate	$cm^{-3} \cdot s^{-1}$
K_{th}	thermophoretic coefficient	
K_{tK}	thermal coagulation coefficient	
Le	Lewis number	
M	mole weight	$kg \cdot kmol^{-1}$
N	number concentration	cm^{-3}
N_P	number concentration of nuclei	cm^{-3}
N_V	volume concentration	$cm^3 \cdot m^{-3}$
p_i	partial pressure	bar
S	degree of saturation	
t	temperature	°C
T	temperature	K
y	mole fraction	
Y	concentration	g vapor·(kg dry gas)$^{-1}$
z	vertical condenser position	cm

Greek symbols

η	dynamic viscosity	$kg \cdot m^{-1} \cdot s^{-1}$
λ	heat conductivity of the gas phase	$W \cdot m^{-1} \cdot K^{-1}$
ρ	density	$kg \cdot m^{-3}$
σ	standard deviation of particle size distribution	
τ	time	s

Subscripts

crit	critical
F	condensate film
G	gas
L	fog limit
P	particle
S	saturated
V	vapor

Superscripts

in	inlet

* Correspondence and reprints.
arne.manthey@sap.com

1. INTRODUCTION

Formation of aerosols or fog can frequently be watched in industrial condensation processes especially during the condensation of solvents in the presence of inert gases like N_2 or air. Aerosols are gas-particle-systems with particle sizes between 0.1 and 10 μm [1]. Due to their small sizes the particles are hard to separate from the gas phase and can be easily carried to subsequent process stages or cause emission problems. In order to avoid these problems in industrial plants it is convenient to consider a possible formation of aerosols during the design step and provide countermeasures. Therefore a profound knowledge of the processes leading to aerosol formation is required.

Depending on the operation conditions during the condensation of a gas/vapor-mixture the bulk gas phase may become supersaturated due to simultaneous heat and mass transfer, which is the basic condition for the formation of fog. The degree of saturation S is defined as the quotient of the actual vapor pressure p_V in the bulk gas phase and the pressure $p_{V,S}(T)$ of the saturated vapor at the same temperature T:

$$S = \frac{p_V(T)}{p_{V,S}(T)} \tag{1}$$

The term vapor (V) comprises all condensable components under the considered process conditions. Fog formation occurs when the degree of saturation S exceeds a critical value S_{crit}. In technical processes the critical saturation is defined as the degree of saturation with the nucleation rate J exceeding a value between 10^4 $cm^{-3}{\cdot}s^{-1}$ and 10^6 $cm^{-3}{\cdot}s^{-1}$ [2, 3]. In the presence of foreign and wettable nuclei in the gas phase, that means in the case of heterogeneous nucleation, the critical saturation amounts to $S_{crit} \approx 1.01$ [1, 4]. In the absence of foreign nuclei homogeneous nucleation takes place at degrees of critical saturation greater than 2 and depends strongly on the temperature and the type of components. For the system air/water in a temperature range from 20 °C to 100 °C the value of the critical saturation lies between 2 and 4 [5]. After nucleation, the particles grow due to the condensation of vapor on the surface of the fog particles resulting in an asymptotic decrease of the degree of saturation until $S = 1$ is reached and the particle growth is stopped.

The magnitude of the degree of saturation depends on the course of the saturation line ($S = 1$) and the process path. The saturation line represents the saturation concentration as function of the temperature $Y_S(t)$. In this work the concentration Y is defined as mass unit (gram) vapor per kilogram inert gas (air). The process path represents the course of concentration as a function of the temperature $Y(t)$ in the bulk of the gas phase. The curve of the process path is governed by the process parameters and the Lewis number Le of the gas/vapor system:

$$Le = \frac{\lambda}{\rho c_p D} \tag{2}$$

Large vapor molecules are less movable which results in a small diffusion coefficient D and therefore in a larger Lewis number. This means that heat transfer is faster than the mass transfer compared to smaller molecules. As a consequence those systems will more likely become supersaturated than systems with smaller molecules (e.g., water).

Colburn and Edison [6] made the first simple experimental investigations on fog formation in condensers and calculated the process path during condensation by combining the balances of mass and energy. In many industrial condensation processes the amount of condensable vapor is small compared to the carrier gas phase (e.g., solvent recovery from exhaust air). Additionally the cooling temperature often remains fairly constant due to high coolant flows or evaporating refrigerants. For small inlet concentrations Y^{in}, constant film temperature t_F of the condensate and constant Lewis number the resulting equation for the concentration–temperature curve may be written as [7]:

$$Y(t) = Y_S(t_F) + \left(Y^{in} - Y_S(t_F)\right)\left[\frac{t - t_F}{t^{in} - t_F}\right]^{Le^{-0,6}} \tag{3}$$

The upper graph of *figure 1* shows the process paths for two inlet conditions (points 1 and 2) for the system air/water ($Le \approx 1$) and a hypothetical system with $Le = 2$ with an identical equilibrium curve ($S = 1$). For $Le = 1$ the process paths become straight lines whereas a higher Lewis number results in upturned curved lines. As a consequence even inlet conditions with a low degree of saturation (e.g., $Y^{in} = 50$ $g{\cdot}kg^{-1}$ and $t^{in} = 70$ °C) may lead to supersaturation in the process course. The respective curves of the saturation degree in the lower graph show, that the magnitude of saturation is higher for higher Lewis numbers and for high inlet concentrations with high saturation (low temperatures). For Lewis numbers below or equal unity a fog limit inlet temperature t_L can be identified for each inlet concentration above which no supersaturation occurs and therefore fog formation is not possible.

The topic covered in this article is the formation and behavior of fog in condensation processes. For this purpose a new experimental setup has been designed and

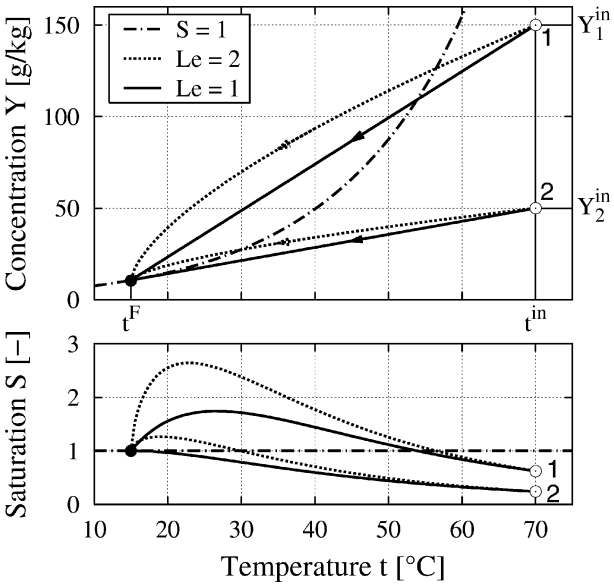

Figure 1. Process paths and degree of saturation for the condensation of gas–vapor-mixtures with various Lewis numbers at inlet conditions $(Y_1, t_{1/2})$ and $(Y_2, t_{1/2})$.

built which allows a view inside a shell and tube condenser. Mixtures of water and air have been used in this work as example for a gas–vapor-system. Given the small Lewis number of a water–air mixture the expected supersaturation is not high enough for homogeneous nucleation. Therefore the main attention has been set on heterogeneous nucleation. Experimental data for various process parameters has been collected. Several different theoretical one- and multidimensional models have been studied and compared with the experimental results. These models include also the particle dynamics along the condenser length. The objective of these investigations is to find means to prevent or reduce fog formation in condensation processes.

2. EXPERIMENTAL

The main component of the new experimental setup is a vertical tube bundle condenser (3) with a double glass shell (*figure 2*). The height of the condenser is 3 m and the inner diameter of the shell comes to 0.1 m. A laser-optical aerosol measurement device using the Three-Wavelength-Extinction Method [8] is mounted on a vertically moveable sled. This allows the determination of the aerosol parameters along the whole length of the condenser. The information obtained by the three-wavelength-extinction method (3-WEM) is the total amount of fog (volume concentration N_V in cm^3 fog per m^3 gas) and the parameters of the particle size distribution assuming a lognormal distribution (number volume averaged diameter d_{NV} and standard deviation σ). Since the theory of the 3-WEM assumes spherical particles this method is especially suited to measure liquid aerosols [9]. The number concentration N is calculated from the volume concentration N_V and the mean particle diameter d_{NV}:

$$N = \frac{6}{\pi} \frac{N_V}{d_{NV}^3} \tag{4}$$

The number concentration N does not necessarily represent the total number concentration N_P of the foreign particles since not all of these particles may serve as condensation nuclei under the given conditions because of insufficient wettability of the particle material.

Due to the temperature decrease in the condenser the specific volume of the gas which serves as reference variable for the concentrations N and N_V is also decreasing. Assuming a constant number of particles per kg air this would lead to a discrepancy between the concentrations in the inlet and outlet of the condenser. In the experiments this discrepancy comes up to 20 %. However this value is relatively small compared to the large influence of particle dynamics discussed later on.

To provide pressurized air for the experiments a compressor is used. A small flow of heated air is piped through the outer shell to prevent condensation of vapor on the inside of the inner shell which would disturb the 3-WEM measurement. To allow fog formation by heterogeneous nucleation the main air stream (solid line) is charged with condensation nuclei being sucked in with a jet pump (1). The nuclei are provided by the smoke of burning incense cones. In a packed column (2) the air is saturated with water at a specified temperature t_S ($Y^{in} = Y_S(t_S)$). Finally, the mixture is heated up to the desired inlet temperature t^{in} and enters the condenser through 4 radial inlets. In the majority of cases the volume flow has been set to 3.5 $m^3 \cdot h^{-1}$, corresponding to a gas velocity of $v = 0.2$ $m \cdot s^{-1}$. The flow of the cooling water has been chosen large enough to ensure a constant cooling temperature between 13 °C and 15 °C. The maximum saturation temperature in the experiments was 70 °C corresponding to an inlet vapor concentration of approximately 265 $g \cdot kg^{-1}$.

Preliminary investigations without addition of condensation nuclei showed no fog formation by homogeneous nucleation even for high vapor concentrations. This conforms with the low magnitude of saturation ($S < 2$) due to the small Lewis number of the system

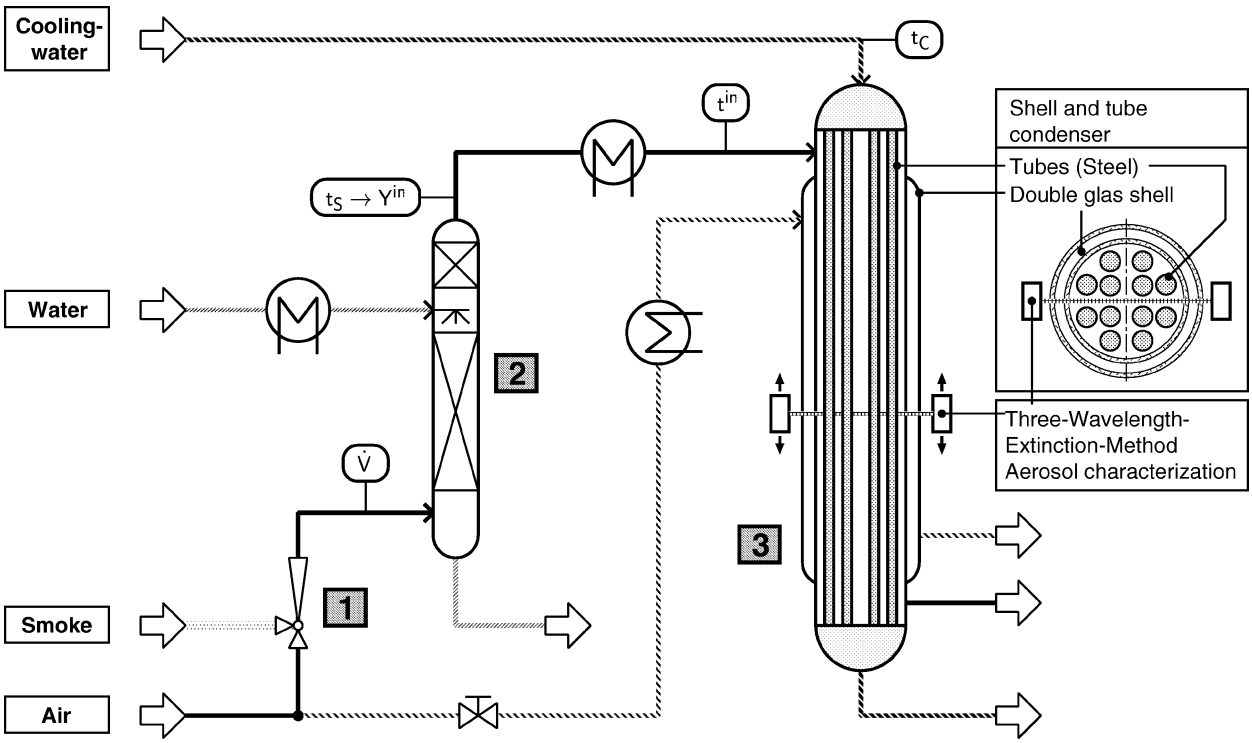

Figure 2. Basic flowsheet of the experimental setup. Jet pump (1), packed column (2), condenser (3).

air/water. As soon as condensation nuclei (smoke) are added to the mixture a strong formation of fog can be observed. The fog is not evenly distributed throughout the cross-section but flows in strands which are temporarily interrupted.

Figure 3 shows the aerosol parameters obtained by 3-WEM measurement at a fixed condenser position for steady state process parameters. After a reference measurement ($\tau = 0$ s) a burning cone is put under the suction inlet of the jet pump. A few seconds later all aerosol parameters have come to a stable value throughout the burning time. After 6 minutes the cone has been removed and replaced by two ignited cones. The doubling of condensation nuclei resulted in a doubling of the number concentration N from roughly $2{\cdot}10^6$–$4{\cdot}10^6$ particles per cm^3. However, the volume concentration N_V representing the total amount of fog remained constant. Steinmeyer [10] reported an increase of fog amount with rising number concentration of foreign nuclei between 10^2 and 10^7 $1{\cdot}cm^{-3}$. For nuclei concentrations above 10^6 $1{\cdot}cm^{-3}$ yet this increase showed to be stagnating.

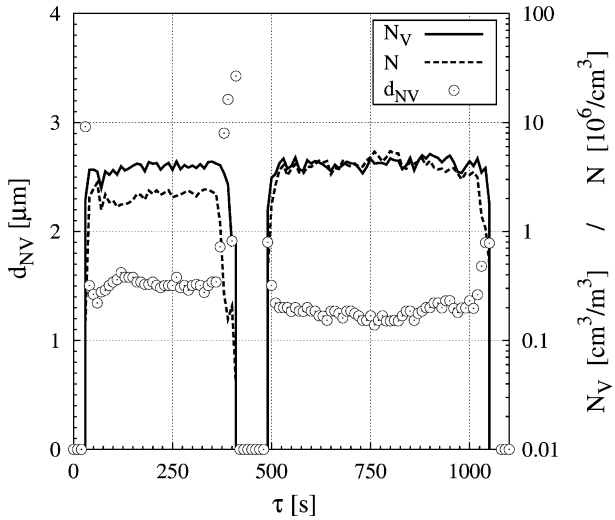

Figure 3. Aerosol parameters of fog formed by heterogeneous nucleation at $Y^{in} = 140$ g·kg^{-1} and $t^{in} = 70$ °C using one incense cone (left side) and two incense cones (right side) as condensation nuclei generators.

In the course of the experimental investigations two objectives have been followed. First, the behavior of the aerosol parameters along the condenser length has been studied for steady state condensation using various inlet conditions. Therefore measurements such as shown in *figure 3* have been made for up to 10 vertical positions of

which the mean values of aerosol parameters have been calculated resulting in one stationary data point each.

Secondly, the effect of inlet temperature and concentration on the total amount of fog has been investigated by dynamic measurements with continuously varying inlet temperatures rising from initial saturation temperature t_S at fixed inlet concentrations. On this occasion the fog limit inlet temperatures have also been identified.

3. SIMULATION

For the interpretation of experimental results the condensation process has been simulated using four models and various calculation tools. The main attention in all models has been set on the degree of saturation as prerequisite condition for fog formation and on particle dynamics such as phoresis and coagulation. *Table I* gives a brief summary of the different types of simulation models used in this work.

For a first approach a one-dimensional model was used considering only the gas phase balances with the film temperature being equal to a constant cooling wall temperature (Simulation 1). The heat and mass transfer has been calculated using the film model including Stefan-flow and Ackermann-correction. In contrast to the model represented by equation (3) the Lewis number is considered to be dependent on temperature and concentration. For this model the condenser geometry has been replaced by a simple shell and tube condenser with the same flow cross-section and cooling area compared to the real geometry (*figure 4*).

To study the process in more detail multi-dimensional simulations have been carried out using the computational fluid dynamics program FIDAP. As before only the gas phase has been described. Two-dimensional simulations (Simulation 2) have been made for the simple geometry according *figure 4* and three-dimensional simulations have been carried out for the real condenser geometry (Simulation 3).

The results, that means the fields of temperature and concentration of these simulations have been used for a post-processing of the particle dynamics (Simulations 1P–3P) neglecting an interaction of the disperse (particles) and the continuous phase. It was assumed that in the inlet all particles have already been formed by nucleation and growth.

First the course of the particles influenced by thermo- and diffusiophoretic forces has been calculated. Particles touching the cooling wall have been regarded as loss decreasing the number concentration *N*. The ther-

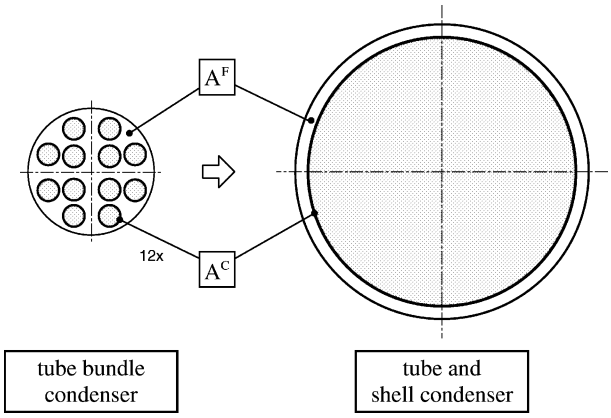

Figure 4. Substitution of the real condenser geometry by a simple shell and tube condenser for one- and two-dimensional modeling.

TABLE I
Summary of the simulation models used in this work.

Type	Description	Geometry	Dimension	Post-processing of particle dynamics	Nucleation and particle growth
(1)	Shell and tube condenser simulation using film model	simple	1	yes (1P)	no
(2)	Shell and tube condenser simulation with FIDAP	simple	2	yes (2P)	no
(3)	Shell and tube bundle condenser simulation with FIDAP	complex	3	yes (3P)	no
(4)	Simulation of condensation in a tube with SENECA	simple	1	no	yes

mophoretic velocity is [11]:

$$\mathbf{v}_{\mathrm{th}} = -K_{\mathrm{th}}(d_{\mathrm{P}})\frac{\eta \,\mathrm{grad}\, T}{\rho T} \tag{5}$$

There are many models in literature for the calculation of K_{th} [12] which lead to values between 0.2 and 1 for particle sizes between 1 and 5 μm. Therefore an average value of 0.5 has been used in this work. The diffusiophoretic velocity can be written as [13]:

$$\mathbf{v}_{\mathrm{diff}} = -\frac{M_{\mathrm{V}}}{yM_{\mathrm{V}} + (1-y)M_{\mathrm{G}}}\,\frac{D\,\mathrm{grad}\, y}{(1-y)} \tag{6}$$

Secondly, the loss of particles by coagulation has been calculated which again leads to a decrease of the number concentration. The rate of thermal coagulation due to Brownian movement is [1]:

$$\frac{\mathrm{d}N}{\mathrm{d}\tau} = -K_{\mathrm{tK}}(T)N^2 \tag{7}$$

For typical particle distributions appearing in the condensation process (median diameter $d_{50} \approx 2$ and geometric standard deviation $\sigma \approx 1.5$) Hinds calculated the coagulation coefficient to:

$$K_{\mathrm{tK}}(T) = 3.5 \cdot 10^{-6}\,\frac{T}{298\ \mathrm{K}} \tag{8}$$

The rate of cinematic coagulation due to velocity gradients can be written as:

$$\frac{\mathrm{d}N}{\mathrm{d}\tau} = -\frac{2}{3}\,\frac{\partial v_z}{\partial x}\,d_{\mathrm{P}}^3 N^2 \tag{9}$$

where $\partial v_z/\partial x$ is the gradient of velocity perpendicular to the direction of the main gas flow.

The formation of particles itself has been considered in the last model (Simulation 4) using the simulation code SENECA (Simulation with Extrapolation methods and Newton techniques of Chemical processes with Aerosol formation) which was developed in our Institute [14, 15]. This code uses a one-dimensional description of continuous gas–liquid contact devices based on energy and mass balances in all participating phases (gas, condensate, cooling water and aerosol droplets) as well as rigorous heat and mass transfer equations, including nucleation and particle growth.

4. RESULTS AND DISCUSSION

Figure 5 shows the typical course of the aerosol parameters along the condenser length during a steady state

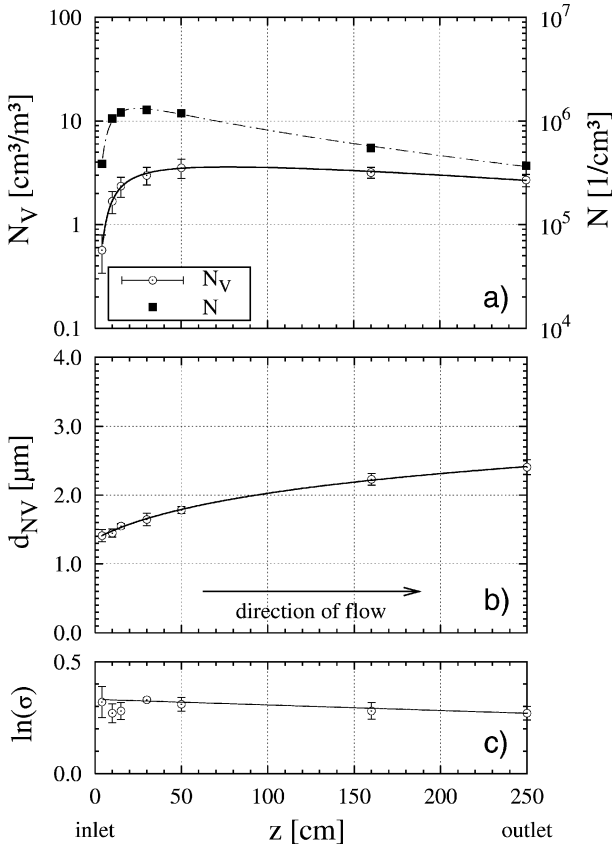

Figure 5. Development of aerosol parameters along the length of the condenser at steady process parameters with inlet concentration 265 g·kg^{-1} and inlet temperature 102 °C.

condensation process. Each point in the graph is the mean value of a 5 minutes measurement while the errorbars represent the degree of fluctuation. In all cases with fog being detected, the formation of fog could be seen with the naked eye at the first contact of humid air with the cooling wall. The standard deviation σ remains fairly constant at a value of 1.5 ($\ln\sigma = 0.4$) whereas the particle size is continuously increasing throughout the condensation process. The volume and number concentration show a more complex behavior which can be divided in two sections:

In the inlet section (0–50 cm) the concentrations N and N_{V} are rising steeply indicating that this section is governed by heterogeneous nucleation and droplet growth. This will be confirmed by the SENECA simulation results later on (see *figure 11*) which show that the formation and growth of fog particles happens during a short residence time (< 1 s).

The outlet section (> 50 cm) shows a stagnation of the volume concentration and — conditional on the simulta-

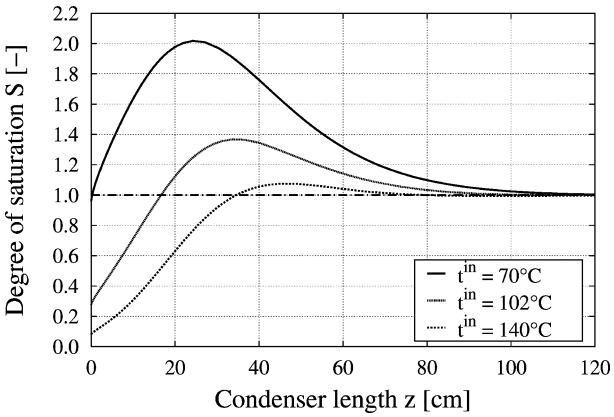

Figure 6. Degree of saturation versus condenser length with an inlet concentration of 265 g·kg^{-1} and various inlet temperatures. One-dimensional simulation results (Type 1) without fog formation.

neous increase of particle size — a strong decrease of the number concentration. The loss of particles can be explained by phoretic forces or coagulation. Since the total amount of fog (represented by the volume concentration) remains fairly constant in this section, it is more likely that coagulation is the decisive mechanism for this decrease.

To investigate the influence of various process parameters several experiments have been carried out for different inlet concentrations ($Y^{\mathrm{in}} = 60$–265 g·kg^{-1}), temperatures ($t^{\mathrm{in}} = 45$–$140\,^{\circ}$C) and volume flows ($\dot{V} = 3.5$–10.5 m^3·h^{-1}). The volume flow has shown not to affect the aerosol parameters. This behavior could be confirmed with one-dimensional simulations (Type 1) which indicate no influence of volume flow on the maximal degree of saturation in the condensation process. The inlet temperature has the strongest influence on the aerosol parameters. With rising temperature a strong decrease of particle size, number concentration and volume concentration has been observed. This can be explained by the evolution of the degree of saturation. In *figure 6* saturation paths are plotted for $Y^{\mathrm{in}} = 265$ g·kg^{-1} and different inlet temperatures. With rising temperature the maximal saturation decreases resulting in a lower rate of fog formation. Above the fog limit temperature ($t^{\mathrm{in}} > 140\,^{\circ}$C) no supersaturation and thus no fog formation occurs.

The one-dimensional simulation results predict that the position in the condenser at which fog starts to form is shifting deeper into the condenser with rising temperature. However, in all experiments the first strands of fog were visible immediately after the air/vapor-mixture has entered the condenser. To solve this discrepancy two- and three-dimensional simulations using FIDAP have been carried out. *Figure 7* shows the degree of saturation in a vertical cross-section of the upper third of a single shell and tube condenser (Simulation type 2). The horizontal axis represents the condenser length from 0 to 1 m and the vertical axis characterizes the split between tube ($r = 108$ mm) and shell ($r = 115$ mm). The cooling wall is located at the bottom of the diagram and the inlet is on the left side. The colored lines represent locations of equal degree of saturation. It is clearly visible that a zone of high supersaturation (red lines) is formed immediately at the inlet near the cooling wall.

This indicates that the formation of fog happens always at the first contact of the mixture with the cooling walls, provided that fog formation is possible at all. *Figure 8* shows the respective three-dimensional simulation result near the inlet at $z = 5$ cm (Simulation type 3). For symmetry reasons it was sufficient to model only one eighth of the tube bundle condenser. As shown before, zones of supersaturation can be seen near the cooling walls.

Naturally, the two- and three-dimensional simulations require a higher computational effort than one-dimensional calculations. The question is whether such an effort is necessary for the characterization of fog formation. *Figure 9* shows the degrees of saturation along the condenser obtained by the different models (Types 1–3). For two- and three-dimensional simulation the saturation has been averaged over the horizontal cross-section. The one-dimensional curve shows a good accordance with the other results. This indicates that one-dimensional calculations are sufficient for the determination of the degree of saturation in a condensation process. Especially the maximal value of the degree of saturation, which is important to answer the question whether or not fog might be formed, can be easily obtained by simple one-dimensional calculations (Type 1).

As pointed out earlier, the number concentration of fog particles decreases strongly after the initial nucleation and growth. This fact has been theoretically investigated considering various mechanisms of particle dynamics mentioned in the previous section. The mechanisms treated in this work are diffusio- and thermophoresis and coagulation due to Brownian movement (thermal coagulation) and flow fields (cinematic coagulation). The influence of these mechanisms on the number concentration is shown in *figure 10*. The volume at standard conditions (1.013 bar and 0 °C) has been used as reference variable for the normalized number concentration N_{N} to avoid an influence of the temperature. The uppermost line shows the influence of thermal coagulation. For each of the next lines another mechanism has been

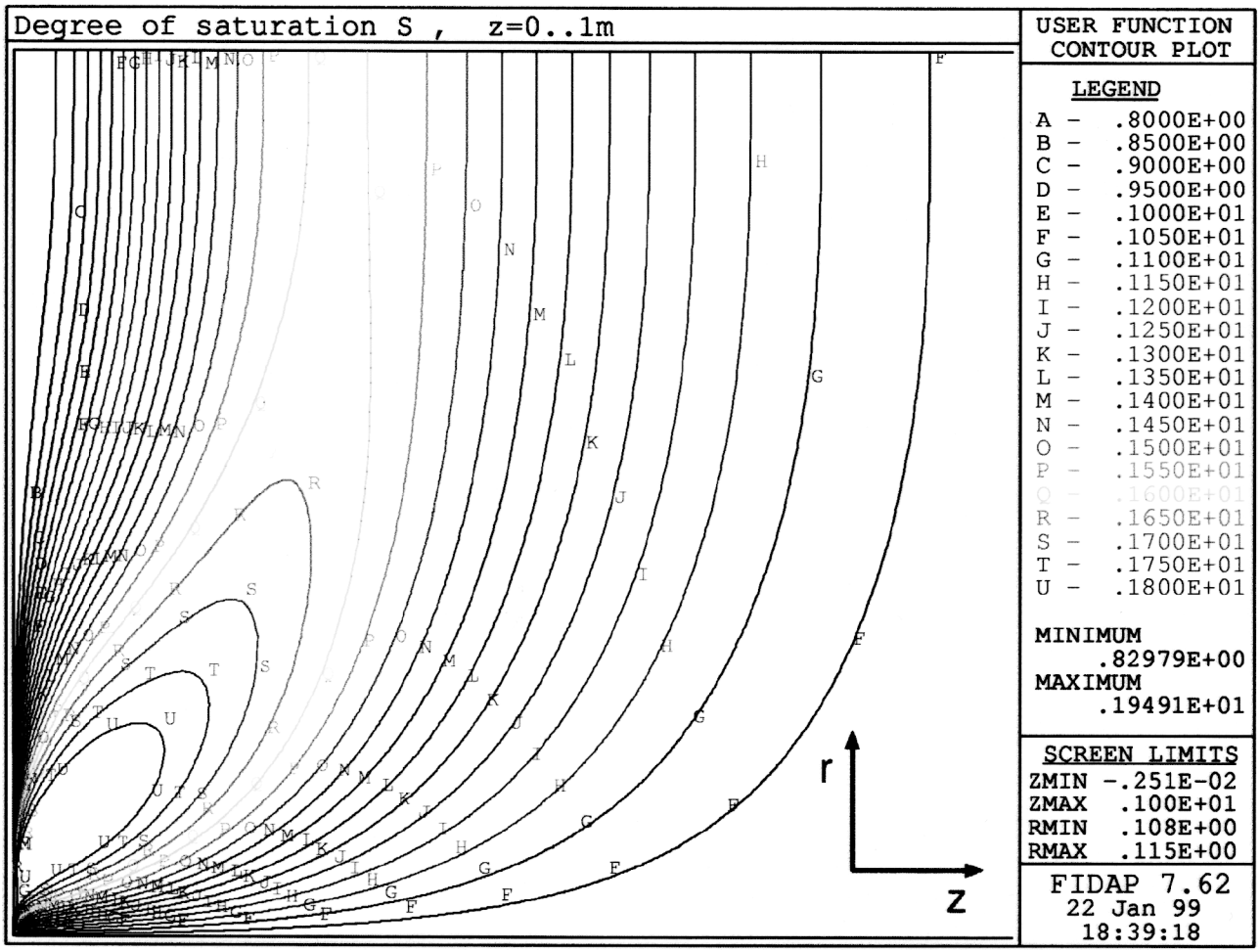

Figure 7. Degree of saturation in a vertical cross-section of a single shell and tube condenser (Simulation type 2). $z = 0$–1 m, $r = 108$–115 mm. $Y^{in} = 200$ g·kg^{-1} and $t^{in} = 70\,°C$.

added. The solid line characterizes the influence of all mechanisms. While coagulation causes a continuous decrease, the influence of phoresis is restricted on the inlet zone where the gradients of temperature and concentration are high enough for a notable effect. However, the simulation results do not correspond with the experimental data marked as solid squares. As mentioned earlier the fog is not uniformly distributed throughout the condenser cross-section. A higher particle concentration in the fog strands might be the reason for a higher rate of coagulation.

The independence of the fog amount on the number concentration of foreign nuclei (*figure 3*) has been confirmed by using the SENECA code (Simulation type 4). *Figure 11* shows the particle diameter d_P and volume concentration N_V as a function of the condenser length z for a varying number concentration N_P of foreign nuclei. The diagrams show that a rising number concentration N_P of foreign nuclei has little effect on the volume concentration but it decreases the fog particle size. The process of fog nucleation and growth is completed after approximately 15 cm which corresponds to a residence time of less than a second.

Since the number of foreign nuclei is seldom known, the fog particle size is hard to predict. However, the volume concentration being a crucial parameter for the characterization of processes with fog formation is rather insensitive to the nuclei concentration and therefore well predictable. *Figure 12* shows the volume concentration as a function of inlet temperature and concen-

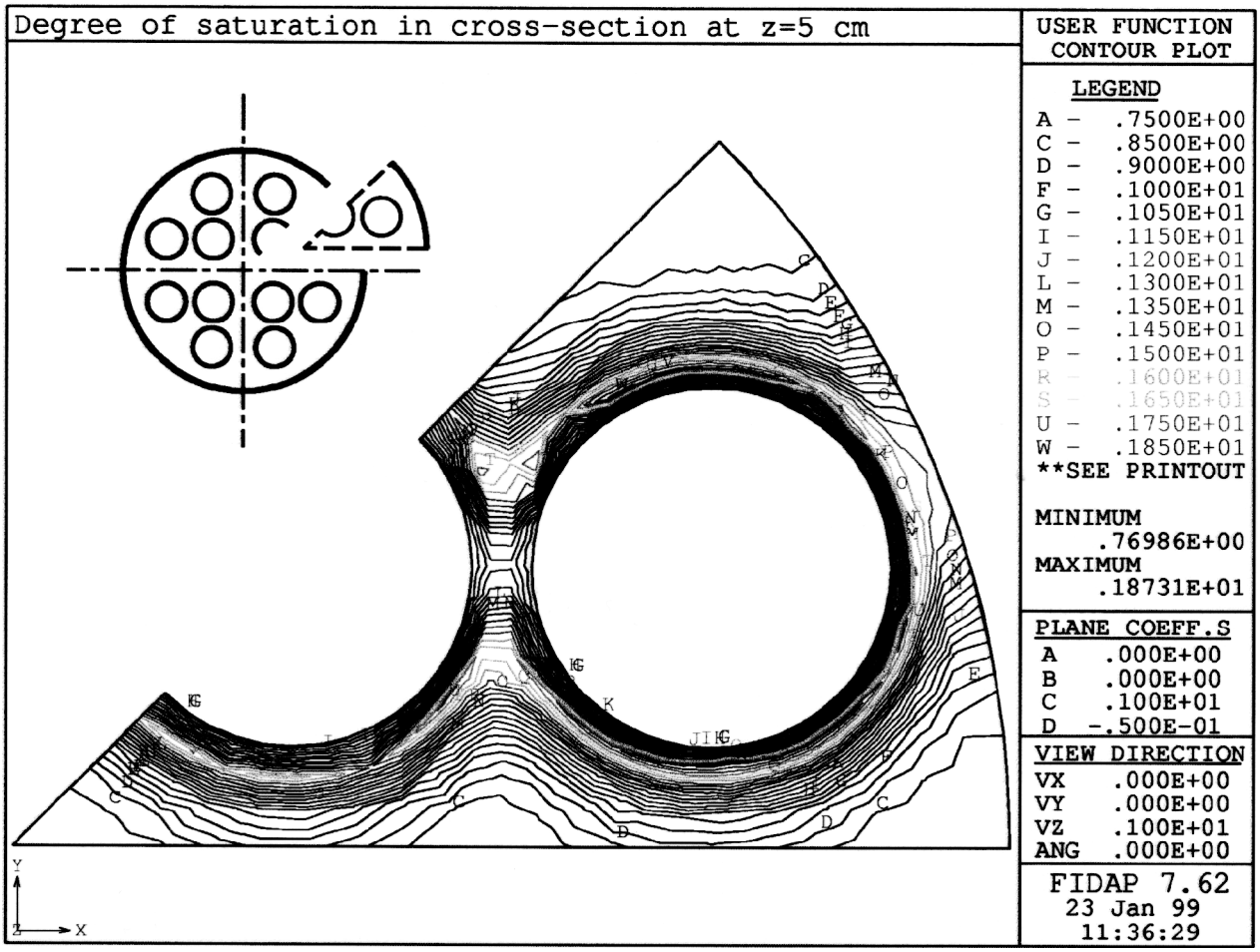

Figure 8. Degree of saturation in a horizontal cross-section of the tube bundle at $z = 5$ cm (Simulation type 3). $Y^{in} = 200$ g·kg^{-1} and $t^{in} = 70\,°C$.

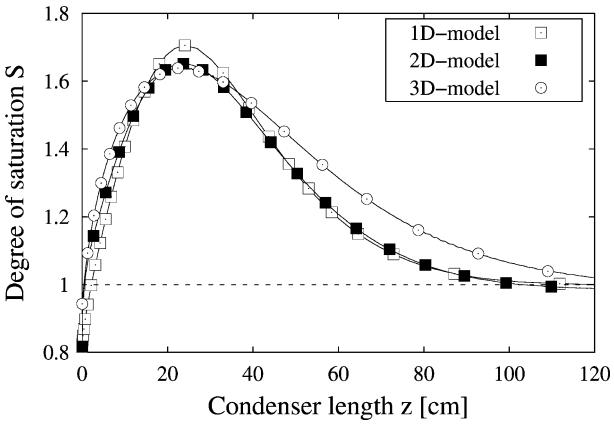

Figure 9. Degrees of saturation along the condenser obtained by different models (Simulation types 1–3). $Y^{in} = 200$ g·kg^{-1} and $t^{in} = 70\,°C$.

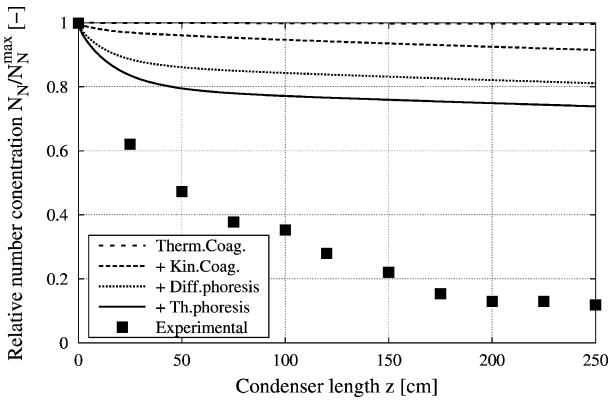

Figure 10. Decrease of particle concentration for $Y^{in} = 200$ g·kg^{-1} and $t^{in} = 94\,°C$. Experimental results and simulations involving various mechanisms of particle dynamics (Simulation type 1P).

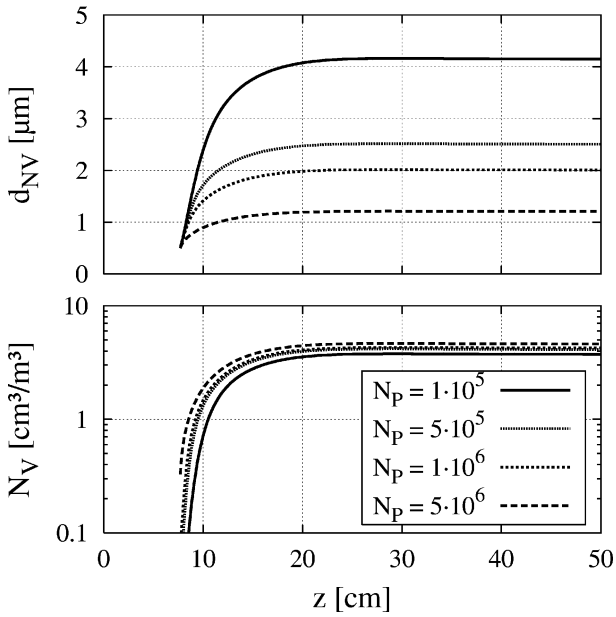

Figure 11. SENECA simulation results (Type 4) of volume concentration and particle size for various concentrations N_P of foreign nuclei. $Y^{in} = 265$ g·kg^{-1} and $t^{in} = 91\,°C$.

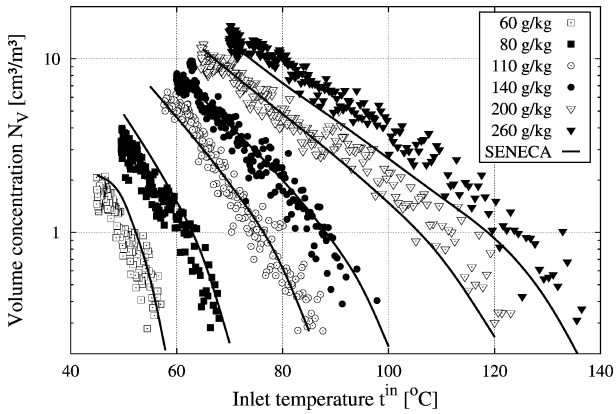

Figure 12. Volume concentration near the condenser inlet ($z = 15$ cm) as a function of the inlet temperature t^{in} obtained with dynamic measurements using various inlet concentrations Y^{in}. Comparison with SENECA simulation results ($N_P = 10^6$ 1·cm^{-3}).

tration obtained by dynamic measurements (symbols) and SENECA simulation (lines). The simulation results match very well with the experimental data. The curves of the volume concentration show an exponential decrease with the inlet temperature and an increase with the inlet concentration. The maximal amount of water (1 cm^3·m^{-3} ≈ 1 g water per kg air) being bound as fog at saturated inlet temperature comes to about 5 % of the inlet concentration.

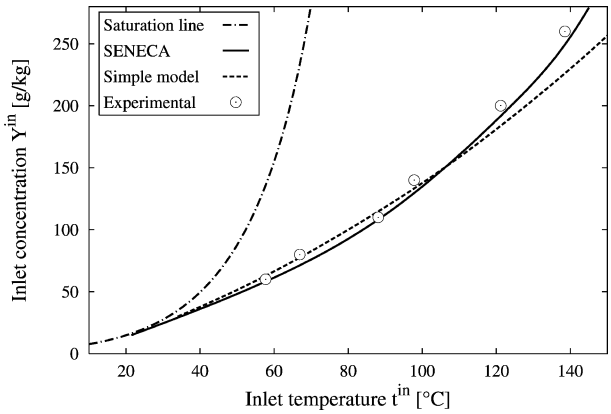

Figure 13. Fog limit as a function of inlet temperature and concentration for a cooling temperature of 15 °C. Experimental and theoretical results.

The highest inlet temperature t_L^{in} at which fog is detectable (fog limit temperature) can be read off for each given inlet concentration. In simulations the fog limit is reached when the maximum degree of saturation becomes unity. In *figure 13* the fog limit is shown as a function of inlet temperature and concentration for a cooling temperature of 15 °C. The solid line represents results of SENECA simulations and the dashed line was obtained by the much simpler one-dimensional model without consideration of fog formation. Both theoretical models are well suited to describe the experimental results (circles) and therefore a rigorous simulation including fog formation (SENECA) is not necessary.

The knowledge of the fog limit is an important criterion for the design and operation of condensers. Inlet conditions above the fog limit line result in fog formation. For inlet conditions below the fog limit no fog will occur. The slope of the fog limit line depends strongly on the cooling temperature. A higher cooling temperature results in a steeper curve whereas a lower cooling temperature leads to a curve with a smaller slope. This fact can be used to prevent fog formation in two-staged condensation processes.

5. CONCLUSION AND SIGNIFICANCE

The formation and behavior of fog in a condenser could be successfully characterized exemplarily for the system water/air with a new experimental setup. The number concentration of foreign nuclei shows no influence on the amount of fog provided that a certain level of number concentration is exceeded. The maximal amount of fog being formed in the condensation process amounts

to 5 % of the inlet vapor concentration. Hence it is not necessary to consider fog formation in the thermal design of a condenser. Despite that two- and three-dimensional simulations showed strong local effects the crucial information of whether or not fog is being formed can be predicted by a simple one-dimensional model. It is also possible to calculate the total amount of fog using a rigorous one-dimensional model including nucleation. These results are expected to be transferable to other systems with a greater technical significance such as organic solvents in air. This will be verified in future investigations.

REFERENCES

[1] Hinds, W.C., Aerosol Technology. Properties, Behavior, and Measurement of Airborne Particles, Wiley, New York, 1982.

[2] Schaber, K., Aerosol formation in absorption processes, Chem. Eng. Sci. 50 (1994) 1347–1360.

[3] Ehrler, F., Schaber, K., Spontane Kondensation und Aerosolbildung, in: VDI-Wärmeatlas/Springer Verlag, 1997, Chapter Je.

[4] Zettlemoyer, A.C., Nucleation, Marcel Dekker, New York, 1969.

[5] Katz, J.L., Ostermier, B.J., J. Chem. Phys. 47 (1967) 478.

[6] Colburn, P., Edison, A.C., Prevention of fog in cooler-condensers, Ind. Eng. Chem. 33 (1941) 457–458.

[7] Schaber, K., Aerosolbildung bei der Absorption und Partialkondensation, Chem. Ing. Tech. 62 (1990) 793–804.

[8] Samenfink, W., Tremmel, A., Dittmann, R., Wittig, S., Schaber, K., Schenkel, A., Multiple wavelength extinction measurements in highly concentrated aerosols under industrial conditions, J. Aerosol Sci. 25 (1994), Special issue, Proceedings of the 1994 European Aerosol Conference.

[9] Schaber, K., Schenkel, A., Zahoransky, R.A., Drei-Wellenlängen-Extinktionsverfahren zur Charakterisierung von Aerosolen unter industriellen Bedingungen, Technisches Messen 61 (1994) 295–300.

[10] Steinmeyer, D.E., Fog formation in partial condensers, Chem. Eng. Progress 68 (1972) 64–68.

[11] Waldmann, L., Schmitt, K.H., Thermophoresis and diffusiophoresis of aerosols, in: Davies, C.N. (Ed.), Aerosol Science, Academic Press, New York, 1966, chapter 6, pp. 137–162.

[12] Manthey, A., Bildung und Verhalten von Nebel in einem Rohrbündelkondensator [online], Ph.D. thesis, University of Karlsruhe, 2000. http://www.ubka.uni-karlsruhe.de/cgi-bin/psview?document=2000/cheming/1

[13] Whitmore, P.J., Meisen, A., Estimation of thermo- and diffusiophoretic particle deposition, The Canadian J. Chem. Eng. 55 (1977) 279–285.

[14] Körber, J., Schaber, K., Ehrig, R., Deuflhard, P., Modelling and simulation of aerosol formation in absorption processes, J. Aerosol Sci. 29 (1998), Special issue, Proceedings of the 5th International Aerosol Conference, 579.

[15] Körber, J., Schaber, K., Modeling of heat and mass transfer with fog formation, in: Proceedings of the 10th International Heat Transfer Conference, Brighton, 1994.